Year: 2013

Myoblasts inhibit prostate cancer growth by paracrine secretion of tumor necrosis factor-α

Stölting, Meline Nogueira Lucena and Ferrari, Stefano and Handschin, Christoph and Becskei, Attila and Provenzano, Maurizio and Sulser, Tullio and Eberli, Daniel

Originally published as:

Stölting, Meline Nogueira Lucena and Ferrari, Stefano and Handschin, Christoph and Becskei, Attila and Provenzano, Maurizio and Sulser, Tullio and Eberli, Daniel. (2013) *Myoblasts inhibit prostate cancer growth by paracrine secretion of tumor necrosis factor-α.* Journal of urology, Vol. 189, H. 5. S. 1952-1959.

Myoblasts inhibit prostate cancer growth b 1 y paracrine secretion of TNF alpha

Name of authors: **Meline N. L. Stölting[1], MD; Stefano Ferrari[2], PhD; Christoph Handschin[3], PhD; Attila Becskei[4], PhD; Maurizio Provenzano[1], MD. PhD; Tullio Sulser[1], Prof.; Daniel Eberli[1]*, MD. PhD**

Name of institutions: [1]Laboratory for Urologic Tissue Engineering and Stem Cell Therapy, Division of Urology, University of Zurich, Frauenklinikstrasse 10, CH 8091 Zurich, Switzerland; [2]Institute of Molecular Cancer Research, University of Zurich, Winterthurerstr 190, CH-8057 Zürich, Switzerland; [3]Biozentrum, Focal Area Growth and Development, University of Basel, Klingelbergstrasse 50-70, CH-4056 Basel, Switzerland; [4]Institute of Molecular Biology, University of Zurich, Winterthurerstr 190, CH-8057 Zürich, Switzerland

Published in J Urol. 2013 May;189(5):1952-9. PMID: 23123370. doi: 10.1016/j.juro.2012.10.071

Title: **Myoblasts inhibit prostate cancer growth by paracrine secretion of TNF alpha**

Name of authors: **Meline N. L. Stölting[1], MD; Stefano Ferrari[2], PhD; Christoph Handschin[3], PhD; Attila Becskei[4], PhD; Maurizio Provenzano[1], MD. PhD; Tullio Sulser[1], Prof.; Daniel Eberli[1*], MD. PhD**

Name of institutions: [1]Laboratory for Urologic Tissue Engineering and Stem Cell Therapy, Division of Urology, University of Zurich, Frauenklinikstrasse 10, CH 8091 Zurich, Switzerland; [2]Institute of Molecular Cancer Research, University of Zurich, Winterthurerstr 190, CH-8057 Zürich, Switzerland; [3]Biozentrum, Focal Area Growth and Development, University of Basel, Klingelbergstrasse 50-70, CH-4056 Basel, Switzerland; [4]Institute of Molecular Biology, University of Zurich, Winterthurerstr 190, CH-8057 Zürich, Switzerland

[*] Corresponding Author: Daniel.Eberli@usz.ch, Phone: +41 44 255 9619, Fax: +41 44 255 9620

Keywords: Prostate cancer growth inhibition, myoblast transplantation for SUI, metastasis hindrance.

Word count (Abstract): 299

Word count (text): 2680 (2381+ 299)

Word count (Take Home Message): 35

ABSTRACT

Background: Myoblasts are capable of forming muscle fibers after transplantation and are therefore envisioned urinary incontinence treatment after radical prostatectomy. However, the safety of this treatment and its interactions with putative remaining neighboring cancer cells has not yet been investigated.

Objective: To determine the safety of myoblast transplantation for the treatment of post-prostatectomy stress urinary incontinence by analyzing microenvironmental interactions between myoblasts and prostate carcinoma cells *in vitro* and *in vivo*.

Design, Setting and Participants: Myoblasts isolated from *rectus abdominis* of patients undergoing abdominal surgery were co-cultured with prostate cancer cells and subcutaneously co-injected with tumor cells *in vivo*.

Outcome Measurements and Statistical Analyses: Cell proliferation, cycle arrest and apoptosis of cancers in co-culture with myoblasts were performed. Tumor volume and metastasis formation were evaluated in a mouse model. Tissue specific markers were assessed by immunohistochemistry, FACS analyses, Western blot and RT-qPCR. Outcome was statistically analysed by independent samples t-tests, one-way-ANOVA and Pearson Correlation.

Results and Limitations: In this study we have demonstrated that myoblasts, in proximity of tumor, provide paracrine TNFα to their microenvironment, decreasing tumor growth of all prostate cancer cell lines examined. Co-culture experiments showed induction of cell cycle arrest, tumor death by apoptosis and increased differentiation of myoblasts. This effect was in large parts blocked by TNFα inhibition. The same outcome was demonstrated in a mouse model, where co-injected human myoblasts also inhibited tumor growth and metastasis formation of all prostate cancer cell lines evaluated. This research is based on established models for cancer research.

However, the complex interactions between stromal and tumor cells were not addressed.

Conclusions: Our results suggest that differentiating MPCs restrict tumor growth and limit metastasis formation by paracrine TNF-a secretion and support the safety of cellular therapy using myoblasts for muscle reconstruction, even in the proximity of prostate cancer.

TAKE HOME MESSAGE

Differentiating MPCs restrict tumor growth and limit metastasis formation by paracrine TNF-a secretion. This Indicates that the treatment of post prostatectomy urinary incontinence with autologous myoblasts is safe, even in patients with recurrent prostate cancer.

INTRODUCTION

Skeletal muscle comprises nearly 50% of the human body, is richly vascularized but rarely the site of cancer metastases. The cellular and molecular mechanisms underlying this phenomenon are not yet understood[1]. An intrinsic protective mechanism avoiding ingrowth of metastatic cells and formation of new tumors seems to be present. Simultaneously, skeletal muscles are the source of myoblasts[2], which are capable of regenerating muscle fibers, and therefore are investigated for the treatment of several muscular dysfunctions, including stress urinary incontinence (SUI)[3], a frequent complication after radical prostatectomy[4]. Preclinical studies have demonstrated that myoblasts, when implanted in the urinary sphincter, efficiently recover continence [5]**.** The pelvic floor is also a frequent site of residual prostate cancer cells[6], but until now no investigations targeted cell fate and possible interactions between myoblasts and vicinal preexisting cancer.

Parallels have long been drawn between stem cells and cancer cells. In fact, both cell types share common features such as capacity for self-renewal, differentiation potential, relative quiescence, resistance to drug and toxins, resistance to apoptosis, secretion of growth factors and stimulation of angiogenesis by production of vascular endothelial growth factor (VEGF)[7]. These features could result in two possible outcomes: Cell proliferation or cell death. For instance, the presence of VEGF, which is secreted by many stem cells and progenitor cells including myoblasts[8], has the potential to promote prostate cancer angiogenesis leading to enhanced tumor growth and bone metastasis[9]. On the other hand, myoblasts are activated by inflammation[2] and use inflammatory cytokines to perform and regulate their cross-talk for activation and differentiation[10]. These same inflammatory cues, paracrine secreted by myoblasts, could triggers cancer apoptosis.

A recent study successfully demonstrated inhibited growth of melanoma cells in the presence of myoblasts, but failed to describe a possible intercellular mechanism that explains this cell behavior [11]. Upon differentiation, myoblasts secrete tumor necrosis factor alpha (TNFα), which plays a key role in myoblast activation and differentiation, thereby linking inflammation to muscle regeneration[12]. In tumor cells, TNFα activates two parallel pathways, nuclear factor-κB (NF-κB) or c-Jun N-terminal kinase (JNK). If NF-κB is activated, TNFα acts as a growth promoter, stimulating proliferation and metastasis. However, if JNK is turned on, a Caspase3-dependent-apoptosis-pathway leads to cell death[13]. In this study, we demonstrate that myoblast-secreted-TNFα is capable of influencing vicinal prostate carcinoma by inducing cell cycle arrest and apoptosis *in vitro* and *in vivo*. Additionally, despite the proximity to prostate cancer, myoblasts will rapidly differentiate into well-organized myotubes. Cell-therapy with myoblasts might provide an ideal treatment of post-prostatectomy urinary incontinence by improving sphincter function and inhibiting potential recurrent prostate cancer in the pelvic floor.

MATERIAL AND METHODS

Cell Isolation and Culture

Upon ethical-approval and informed-consent, myoblasts were isolated from *rectus abdominis* biopsies of male patients (60-80 y) undergoing abdominal surgery. Biopsies were immediately processed according to established protocols[14] and cells were expanded until passage 2 (P2) with a medium change every third day. Cell characterization was performed by cellular growth rate, FACS analyses, Immunocytochemistry, gene expression assay (RT-QPCR) and Western Blot. Muscle tissue formation was assessed by injecting 5 million myoblasts with a collagen carrier into the subcutaneous space of nude-mice. Tissues were retrieved after three and six weeks for histological analysis.

The three prostate carcinoma cell lines (ATCC-LGC Standard) were chosen according to their increasing clinical aggressiveness. They are retrieved from lymph node (LNCaP)[15], bone (PC3) [16], and brain (DU145) metastasis[17]. An aggressive vulvar leiomyossarcoma cell line (SK-LMS1) served as an additional cancer control [18]. An indirect co-culture model (BD Falcon™) was applied, where cells shared culture medium (DMEM enriched with 10% fetal bovine serum (FBS) and 1% streptomycin/penicillin) thereby exchanging their cellular products without direct cell-cell-contact. Cells were co-cultured for 10 day with medium change every third day, and analyses performed at four time points (days 1, 4, 7 and 10). TNFα was neutralized with a mouse monoclonal anti-TNFα antibody (Sigma, T-6817).

Growth Rate and Fiber Formation Assay (FFA)

Cells were trypsinized and hemocytometer cell counts were performed on triplicates,

averaged and growth curves were plotted by time (days). In all cases, triplicate samples of log phase cells were plated at a density of $5x10^3$cells/cm^2. Cell viability was confirmed by toluidine blue staining. The formation of myofibers was examined on slide chambers and after 8 days in differentiating condition myofibers were fixed (methanol, 7min), stained (1:20 Giemsa, 1h) and air dried. Images were taken with a Leica-Imager-M1 Microscope. Five high-power-fields (HPF) were analyzed and data expressed as fused cells in myofibers/HPF, number of fibers/HPF and cells per fiber.

FACS Analyses

Cells were immunolabeled by overnight incubation with anti-Pax7 (1:200,Sigma), anti-MyoD (1:100,BDPharmingen), anti-desmin (1:50,BDBiosciences), anti-MyHC (1:4,DSHB) and anti-sarcomeric-α-actinin (1:1000,Sigma) and one hour with FITC-Goat-Anti-mouse-IgG/IgM antibody (2ng/μl,BDBiosciences). A total of 50'000 events were recorded by FACSCanto flow-cytometer (BDBiosciences) immediately after labeling and data analyzed using FlowJo (7.1.3,Tree Star Inc.). All data are expressed as percent positive cells as defined by flow-cytometry.

Western Blot

Cells were washed with PBS/protease inhibitor (Sigma) and lysed with lysis buffer (50mM Tris-HCl, 150mM NaCl, 10% glycerol, 1% Triton X-100, 2mM EDTA, 40mM ß-glycerophosphate, 50mM sodium-fluoride, 10µg/ml leupeptin, 10µg/ml aprotinin, 1µM pepstatinA, 1mM PMSF). Samples were centrifuged (10min, 13000rpm), and proteins determined in the supernatant. Total protein was measured using DC™ Protein-Assay (Bio-Rad), and 30 µg of protein lysate was loaded on 12% Biorad gels. Proteins were transferred onto PVDF-membranes (Millipore), blocked (1h, 5% non-

fat-dry-milk), and incubated (4°C, overnight) with anti-Desmin (1:100,BD Biosciences), anti-MyH (1:6,DSHB), anti-TNFα (1:500,Sigma), anti-$p21^{WAF1}$ (1:1000,Calbiochem), Cleaved Caspase-3-Asp175 (1:1000,Cell- Signaling) and anti-GAPDH (1:2000,Sigma). Membranes were washed (TBS-0.1% Tween-20, 30min), incubated with HRP-conjugated secondary antibody (TBS-0.1% Tween-20, 5% non-fat-dry-milk, 1 h) and developed by an ECL-technique (ECL-Kit, Amersham).

RT-qPCR

RNA extraction, cDNA preparation and RT-qPCR reactions were done using Taqman® gene expression assay kits (Applied Biosystems), according to manufacture's protocols. Data were normalized with 18S expression, quantitatively analyzed by quantification cycles (C_q) and fold changes[19] and graphically represented in amplification plots. MIQE guidelines were followed.

In vivo Experiments and Tumor Size Determination

Myoblasts and tumor cells were cultured as described above, mixed in a collagen carrier (1mg/ml) and bilaterally injected into the dorsal subcutaneous space of 8 nude-mice (i.e. 16 samples) per group. Cell-cell interactions *in vivo* were examined on day 21 and 42 after injection in nine groups: four with co-injected $5x10^6$ myoblasts and $2.5x10^6$ cancer cells (LNCaP, PC3, DU145 and SK-LMS), four controls of the respective tumors with $2.5x10^6$ cancer cells alone, 1 myoblast control with $5x10^6$ cells. The experiments were performed in time course triplicates and repeated with four different patient myoblasts samples. Tumor volume and growth was measured and volume was calculated according to the formula $mm^3=a^2xb/2$ [20]. Tumor/sample size, myoblast differentiation, tumor aggressiveness and metastasis (lymph node,

lung and liver) were assessed after three and six weeks by histological staining of 10 μm thick frozen sections. Histomorphometric analysis was performed using the MBF software “IMAGEJ for microscopy”.

Histological Staining and Immunocytochemistry

Cells/tissues were fixed (4% PFA,10min, RT), permeabilized (0,5% Triton, 7min), blocked (5% BSA/0,1% Triton, RT, 30min) and immunolabelled with anti-Pax7 (1:200,Sigma), anti-MyoD (1:100,BDPharmingen), anti-desmin (1:50,BDBiosciences), anti-MyH (1:4,DSHB) and anti-sarcomeric actinin (1:1000,Sigma), and incubated 1 hour with anti-mouse-IgG-Cy3 (Sigma). Digital images were taken with a Leica Imager M1 Microscope. Tissues were also stained with Hematoxylin and eosin (HE) by incubating slides in hematoxylin (10min, water rinse 2min), dipping in 1% acid alcohol and Eosin, and dehydrating with consecutive EtOH (70%, 96%, 100%) and Xylol dips.

Statistics

Presented data are expressed as averages with corresponding standard deviation. Analyses by independent samples t-tests, one way ANOVA or Pearson Correlation were done with SPSS v20 (SPSS Inc, Chicago, IL). Graphics were drawn on the GraphPad software Prism 5 for Windows. A $p<0.05$ was considered significant.

RESULTS

Myoblasts differentiate and cancer cells undergo cell cycle arrest and apoptosis in co-culture *in vitro*

Human myoblasts were successfully isolated and characterized by FACS, Immunocytochemistry (ICC) and Fiber Formation Assay (FFA). The cell population expressed 76.5 ± 2.3% PAX-7, 60.6 ± 6.3% MyOD, and 81.6 ± 2.5% desmin. After four days of co-culturing human myoblasts (Figure 1A, 1B) and prostate carcinoma cell lines *in vitro* (Figure 1C, 1D), myoblasts displayed a decreasing growth rate (Figure 1E), fused and developed muscle fibers and, therefore increasing (Figure 1F) their differentiation ratio ($p<0.001$). While only 4.2 ±1.0% of the control myoblasts formed muscle fibers, the differentiation ratio of myoblasts increased in parallel to the respective prostate cancer line aggressiveness ($p=0.011$), with rates of 11.5 ±5.5% in LNCaP, 14.5 ±6.9% in PC3 and 25.3 ±2.3% in DU145. Conversely, cancer cell lines significantly decreased ($p<0.001$) their growth rate (Figure 1G). The decrease in cancer cell growth was due to cell cycle arrest and apoptosis (Figure 1H), as demonstrated by Western Blot and RT-QPCR for Caspase 3 and $p21^{WAF}$.

TNFα-dependent induction of cell cycle arrest and apoptosis in cancer cell lines co-cultured with myoblasts.

Myoblasts demonstrated a striking, up to 25 fold, increase of TNFα mRNA when exposed to tumor (Figure 2A), which lead to significantly higher amounts of TNFα ($p<0.001$) into the conditioned-medium in the co-culture system (Figure 2B). The myoblast-TNFα-secretion in co-culture increased gradually according to the corresponding prostate carcinoma aggressiveness ($p<0.001$), significantly correlating (Pearson: 0.754, $p<0.001$) with the myoblast differentiation ratio (Figure 2C). Yet, the

presence of prostate cancer induced higher autocrine-TNFα-secretion by myoblasts, leading to robust muscle fiber formation. Furthermore, TNFα-antibody blocking decreased the myoblast differentiation ratio and permitted cancer growth *de novo* (Figure 2D) by reducing Caspase3 and $p21^{WAF}$ mRNA and protein expression to control-levels (Figure 2E). The myoblast-secreted-TNFα concentration negatively correlated to cancer cell growth ($p<0.001$, Pearson value -0.58) suggesting that myoblast-paracrine-TNFα is sufficient to induce significant cancer growth inhibition. A parallel assay demonstrated that cancer cell lines alone do not reach detectable levels of TNFα RNA or protein expression.

Myoblast restrain tumor growth inducing cancer apoptosis and cell cycle arrest *in vivo*

Interactions between myoblasts and prostate cancer were further investigated *in vivo* by co-injecting myoblasts and tumor cells subcutaneously in nude-mice (Figure 3A). All co-injected samples reduced tumor growth ($p<0.05$), while tumor injected alone kept growing widely (Figure 3A, 3B). Although, no systemic metastasis could be detected, prostate carcinoma infiltrated local lymph nodes (Figure 3C). Lymph node micrometastasis were significantly reduced in co-injected groups (10,9%), when compared to control (90,6%).These results demonstrate that myoblasts collaborate to restrict prostate cancer to its primary site, thus significantly ($p<0.001$) reducing metastasis.

The extent to which myoblasts influenced cancer occurred gradually again following cancer aggressiveness (Figure 4). Histomorphometric distance analyses demonstrated that the tumor areas closer to the newly formed muscle underwent apoptosis and cell cycle arrest more intensely (Pearson values -0.91 and -0.86 respectively) supporting the hypothesis that soluble factors are responsible for the

antitumor effects (Figure 5). Despite the evident changes in tumor behavior, muscle tissue developed a well-organized and differentiated structure *in vivo*. We could not detect any changes in muscle phenotype in the presence of tumor, which also preserved a similar expression of Desmin and $p21^{WAF}$.

DISCUSSION

Cell-cell interactions play a crucial role in tissue formation, regeneration processes and inflammatory reactions. Cellular signalling between neighboring cells is based on two main mechanisms: Growth modulation by endogenous secretion of active compounds and cell competition. These two mechanisms have been well documented in fibroblasts, which are capable of secreting growth factors and other peptides, thus delivering cues to neighboring cells. Fibroblasts isolated from breast tumoral areas are permissive allowing breast cancer metastasis, whereas fibroblast from normal breast tissue restrict tumor growth[21]. Cell competition has also been proposed to regulate early cancer stages, when developing cancer cells overcome genomic constraints[22]. It triggers apoptosis within and around tumors by promoting rivalry between different anaplastic and normal cell lineages[23].

In this context, myoblasts also present key intercellular signaling products that allow cross-talk required for myogenesis and new fiber formation upon muscle injury[24]. We demonstrated that myoblasts produce increased TNFα levels in the presence of tumor cells, stimulating muscle differentiation and inducing cancer cell death. Myoblasts secrete higher TNFα levels when differentiating and this paracrine-secretion evokes microenvironmental changes, which control muscle regeneration by activating Pax7 in quiescent myoblasts and thereby induce differentiation and muscle formation[12]. We have demonstrated that myoblasts in co-culture with cancer cells increaseTNFα-secretion, inducing apoptosis *in vitro* and *in vivo*. TNFα bound to TNFR-1 receptor triggers Caspase-3 activation leading to an apoptotic cascade and cell death[25]. The dual effect of TNFα inducing differentiation in myoblasts and apoptosis in tumors can be explained by two parallel pathways: activation of p38α and c-Jun N-terminal kinase (JNK). Once p38α is activated, Pax7 initiates

myogenesis and myoblast differentiation[12] and, by activating the JNK pathway, triggers cancer apoptosis through a Caspase-3-dependent pathway[13]. A further line of action of TNFα in cancer inhibition affects tumor vascularity, probably due to higher response to TNFα in tumoral vessels by receptor up-regulation (TNFR-1)[25]. These observations suggest that small amounts of TNFα delivered by differentiating myoblasts can be enough to induce tumoral anti-vascular effects.

This research was based on established models for cancer research, however the complex interactions between stromal and tumor cells were not addressed. We demonstrated that myoblast-secreted-TNFα levels increase according to tumor aggressiveness, in accordance with previous findings correlating prostate cancer Gleason-score and inflammatory response to endogenous cytokines[26]. The presence of inflammatory factors related to muscle regeneration plays a role in myoblast-secreted-TNFα regulation[12]. This leads to the hypothesis that specific inflammatory cues delivered by the prostate tumor stimulate neighboring myoblasts to produce higher TNFα levels. A potential pathway is the increase of TACE production due to stress and nutrient shortage, leading to increased release of endogenous TNFα by muscle cells [27]. We anticipate that investigations targeting cancer-mediated-stress factors on muscle cells will be the focus of future efforts towards a better understanding of interactions between cancer and Adult Stem Cells, such as myoblasts.

CONCLUSIONS

Myoblasts can be isolated from muscle biopsies of patients, rapidly grown in culture, implanted into the site of injury and thereafter form functional muscle within weeks. Our results indicate that differentiating myoblasts secret TNFα inducing apoptosis and cell cycle arrest in Prostate cancer. These characteristics make myoblasts promising cell source for muscle reconstruction, even in the proximity of cancer.

ACKNOWLEDGEMENTS

We gratefully acknowledge the technical assistance of Dr. Marten Schneider, Dr. Irina Agarkova, Dr. Sousan Salemi and Fatma Kivrak on the improvement of our FACS, IHC and WB methods. This work was supported by the Hartmann-Müller Foundation, Forschungskredit, Swiss National Foundation and University of Zürich.

REFERENCES

[1] Plaza JA, Perez-Montiel D, Mayerson J, Morrison C, Suster S. Metastases to soft tissue. Cancer. 2008;112:193-203.
[2] Gopinath SD, Rando TA. Stem Cell Review Series: Aging of the skeletal muscle stem cell niche. Aging Cell. 2008;7:590-8.
[3] Carr L, Steele D, Steele S, et al. 1-year follow-up of autologous muscle-derived stem cell injection pilot study to treat stress urinary incontinence. International Urogynecology Journal. 2008;19:881-3.
[4] Klingler HC, Marberger M. Incontinence after radical prostatectomy: surgical treatment options. Current Opinion in Urology. 2006;16:60-4.
[5] Eberli D, Aboushwareb T, Soker S, Yoo JJ, Atala A. Muscle Precursor Cells for the Restoration of Irreversibly Damaged Sphincter Function. Cell Transplantation. 2012.
[6] Leventis AK, Shariat SF, Slawin KM. Local Recurrence after Radical Prostatectomy: Correlation of US Features with Prostatic Fossa Biopsy Findings1. Radiology. 2001;219:432-9.
[7] Reya T, Morrison SJ, Clarke MF, Weissman IL. Stem cells, cancer, and cancer stem cells. Nature. 2001;414:105-11.
[8] Mac Gabhann F, Ji JW, Popel AS. VEGF gradients, receptor activation, and sprout guidance in resting and exercising skeletal muscle. J Appl Physiol. 2007;102:722-34.
[9] Carducci MA, Jimeno A. Targeting Bone Metastasis in Prostate Cancer with Endothelin Receptor Antagonists. Clin Cancer Res. 2006;12:6296s-300.
[10] Dhawan J, Rando TA. Stem cells in postnatal myogenesis: molecular mechanisms of satellite cell quiescence, activation and replenishment. Trends in Cell Biology. 2005;15:666-73.
[11] Parlakian A, Gomaa I, Solly S, et al. Skeletal Muscle Phenotypically Converts and Selectively Inhibits Metastatic Cells in Mice. PLoS ONE. 2010;5:e9299.
[12] Palacios D, Mozzetta C, Consalvi S, et al. TNF/p38[alpha]/Polycomb Signaling to Pax7 Locus in Satellite Cells Links Inflammation to the Epigenetic Control of Muscle Regeneration. Cell stem cell. 2010;7:455-69.
[13] Wang X, Lin Y. Tumor necrosis factor and cancer, buddies or foes[quest]. Acta Pharmacol Sin. 2008;29:1275-88.
[14] Eberli D, Soker S, Atala A, Yoo JJ. Optimization of human skeletal muscle precursor cell culture and myofiber formation in vitro. Methods. 2009;47:98-103.
[15] Horoszewicz JS, Leong SS, Kawinski E, et al. LNCaP Model of Human Prostatic Carcinoma. Cancer Research. 1983;43:1809-18.
[16] Kaighn ME, Narayan KS, Ohnuki Y, Lechner JF, LW. J. Establishment and characterization of a human prostatic carcinoma cell line (PC-3). Investigative Urology. 1979;17:16-23.
[17] Stone KR, Mickey DD, Wunderli H, Mickey GH, DF. P. Isolation of a human prostate carcinoma cell line (DU 145). International journal of cancer. 1978;21:274-81.
[18] Fogh J FJ, Orfeo T. One hundred and twenty-seven cultured human tumor cell lines producing tumors in nude mice. Journal of the National Cancer Institute. 1977;59:221-8.

[19] Schmittgen TD, Livak KJ. Analyzing real-time PCR data by the comparative C(T) method. Nat Protoc. 2008;3:1101-8.
[20] Eva Corey, Janna E. Quinn, Kent R. Buhler, et al. LuCaP 35: A new model of prostate cancer progression to androgen independence. The Prostate. 2003;55:239-46.
[21] Dong-LeBourhis X, Berthois Y, Millot G, et al. Effect of stromal and epithelial cells derived from normal and tumorous breast tissue on the proliferation of human breast cancer cell lines in co-culture. Int J Cancer. 1997;71:42 - 8.
[22] Simpson P, Morata G. Differential mitotic rates and patterns of growth in compartments in the Drosophila wing. Developmental Biology. 1981;85:299-308.
[23] Moreno E. Is cell competition relevant to cancer? Nat Rev Cancer. 2008;8:141-7.
[24] Chen S-E, Gerken E, Zhang Y, et al. Role of TNF-{alpha} signaling in regeneration of cardiotoxin-injured muscle. Am J Physiol Cell Physiol. 2005;289:C1179-87.
[25] van Horssen R, ten Hagen TLM, Eggermont AMM. TNF-{alpha} in Cancer Treatment: Molecular Insights, Antitumor Effects, and Clinical Utility. Oncologist. 2006;11:397-408.
[26] Nuñez C, Cansino JR, Bethencourt F, et al. TNF/IL-1/NIK/NF-kappaB transduction pathway: a comparative study in normal and pathological human prostate (benign hyperplasia and carcinoma). Histopathology. 2008;53:166-76.
[27] Zhan M, Jin B, Chen S-E, Reecy JM, Li Y-P. TACE release of TNF-{alpha} mediates mechanotransduction-induced activation of p38 MAPK and myogenesis. J Cell Sci. 2007;120:692-701.

FIGURE LEGENDS

Figure 1 – **Co-culture effects on myoblasts and cancer cells.** Cell growth rate, differentiation ratio, morphology and gene expression were influenced by co-culture. Myoblasts differentiated rapidly in the presence of tumor, significantly increasing differentiation ratio (A, B, F) and, consequently, decreasing cell growth (E). Prostate carcinoma and sarcoma cells significantly decreased in growth (C, D, G) and underwent apoptosis and/or cell cycle arrest (C, D, H). Desmin staining in co-culture (A) and control (B), Caspase 3 staining of DU145 cells in co-culture with myoblasts (C) and control (D), cytoskeleton labelled in green (Phalloidin 488) and secondary antibody in red (Cy3). Caspase 3 and p21 mRNA fold increase and protein expression (H) significantly increased when compared to tumor control (dashed line=1.0). Samples in co-culture with myoblast were represented as (+ Mb) and control without myoblasts as (- Mb). mRNA fold increase was normalized with 18S reference gene (*$p<0.001$, **$p=0.005$, ***$p=0.011$)

Figure 2 – **Myoblast secreted TNFα induce myoblast differentiation and inhibit cancer cell line growth rate by inducing apoptosis and cell cycle arrest.** (A) RT-QPCR assay demonstrates myoblast mRNA expression increase on the fourth day of co-culture with different cancer cell lines. A significant difference could be found between different prostate cancer cell lines, increasing according to tumor aggressiveness. (B) Myoblasts TNFα secretion increases according to the cancer aggressiveness in co-culture. CM: conditioned Medium. (C) Myoblast differentiation ratio correlate (Pearson correlation: 0.754) to the amount of produced TNFα . (D)

Cell growth rate of cancer (LNCaP, PC3, DU145 and SK.LMS-1) was assessed by cell counting at day 1, 4, 7 and 10 of co-culture. All cancer cell lines showed a significant decrease in growth in the presence of myoblasts (bold lines), when compared to control (fine line). Cancer growth rate was in great part recovered (dashed lines) after TNFα neutralization. (E) Apoptosis and cell cycle arrest are triggered in all cancer cells co-cultured with myoblasts. Again TNFα blocking in conditioned medium reverse in great part these effects. Caspase 3 and p21 tumor control mRNA fold increase is represented with a dashed line (=1.0). (*p<0.001, **p<0.05).

Figure 3 – **Tumor growth and lymph node metastasis was reduced *in vivo* in samples co-injected with myoblasts.** (A) 21 days after subcutaneous cell injection, tumor size was measured and a significant tumor size difference was found between co-injected and control samples. On day 42, myoblast co-injected tumor mass shrank, whereas control samples kept growing. (B) Final tumor size at day 42 was significantly smaller in myoblast co-injected samples. (C) Axillar lymph node metastasis assessment was performed by analysis of macro- and micrometastasis with H&E, Desmin and cytokeratin staining, positive lymph nodes. Ratio of axillar metastasis was also significantly reduced (p<0.001) in all tested cancers, when co-injected with myoblasts. Samples co-injected with myoblasts were represented as (+ Mb) and control without myoblasts as (- Mb). *p<0.05, **p=0.009, ***p=0.002

Figure 04 – **Histological aspect of subcutaneously injected tumor *in vivo*.** At day 42, HE staining demonstrates a tendency of newly formed muscle and cancer tissue (first row) to growth in clusters, with differentiated muscle areas impairing growth of

neighbor tumor masses. In opposition, control cancers (second row) grow freely forming bigger and complex tumor masses. Increasing Caspase3 and $p21^{WAF}$ expression was detected in all tumors in samples co-injected with myoblasts. Samples co-injected with myoblasts were represented as (+ Mb) and controls are cancer cell lines injected without myoblasts (-Mb). In the co-injected samples muscle is represented with a “M” and cancer tissue areas with a “C”. DAPI (blue), anti-mouse IgG Cy3 (red), and the injected myoblasts were labelled *in vitro* with PKH 67 (green). Muscle on

Figure 05 – **Histomorphometric analyses of co-injected tumor with myoblasts.** Histomorphometric analysis demonstrates a significant increase on apoptosis (A) and cell cycle arrest (B) in all tested tumors. (C) Three tumor areas were analyzed according to distance of newly formed muscle. The total positive area, calculated by fluorescence intensity, demonstrated a gradient of Caspase 3 and p21 expression in all cancers tested. These directly correlated with the proximity to differentiating muscle tissue. Samples co-injected with myoblast were represented as (+ Mb) and control without myoblasts as (- Mb). *p<0.001, ** p< 0.05, ***p=0.001

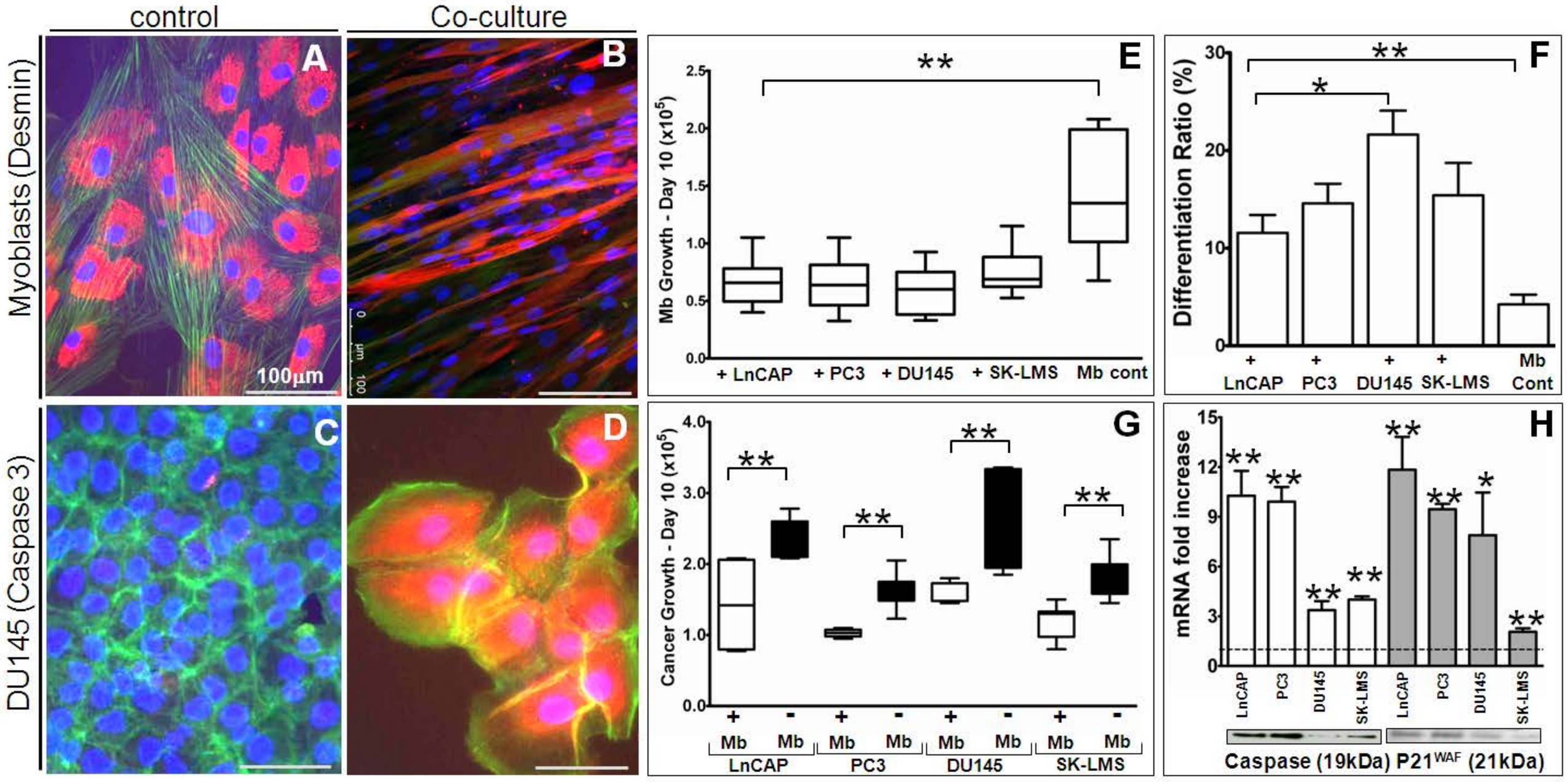
control
Co-culture
Myoblasts (Desmin)
DU145 (Caspase 3)
A
B
C
D
100µm
E
Mb Growth - Day 10 (x10^5)
+ LnCAP
+ PC3
+ DU145
+ SK-LMS
Mb cont
F
Differentiation Ratio (%)
LnCAP
PC3
DU145
SK-LMS
Mb Cont
G
Cancer Growth - Day 10 (x10^5)
Mb
LnCAP
PC3
DU145
SK-LMS
H
mRNA fold increase
Caspase (19kDa) P21WAF (21kDa)

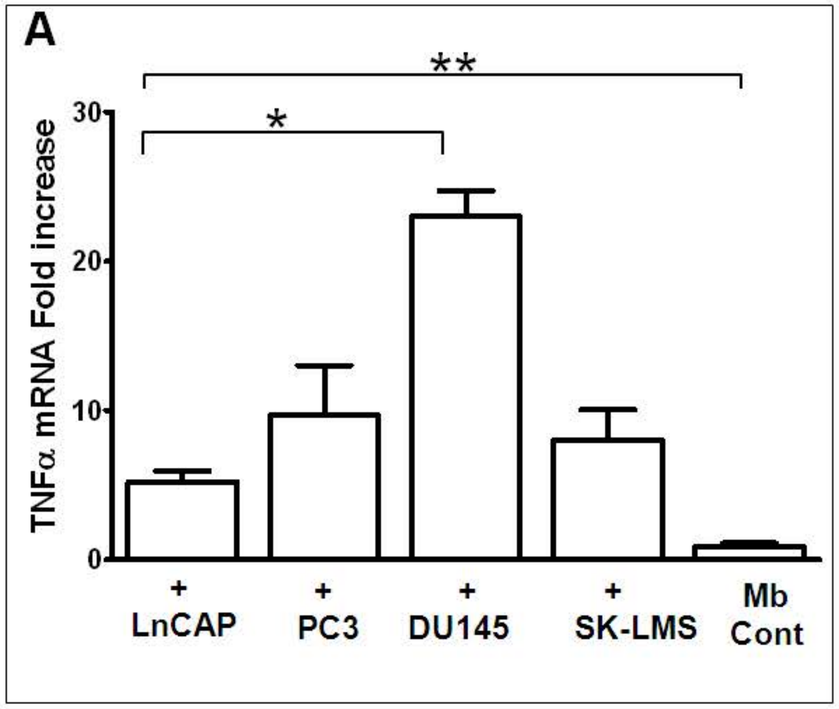
A
TNFα mRNA Fold increase
30
20
10
0
*
**
+ LnCAP
+ PC3
+ DU145
+ SK-LMS
Mb Cont

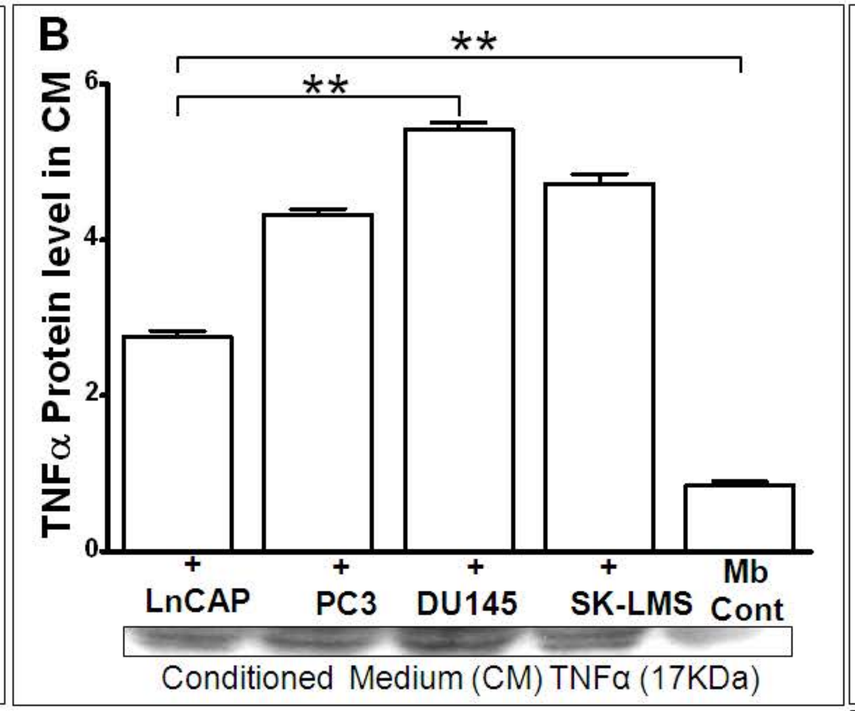
B
TNFα Protein level in CM
6
4
2
0
**
**
+ LnCAP
+ PC3
+ DU145
+ SK-LMS
Mb Cont
Conditioned Medium (CM) TNFα (17KDa)

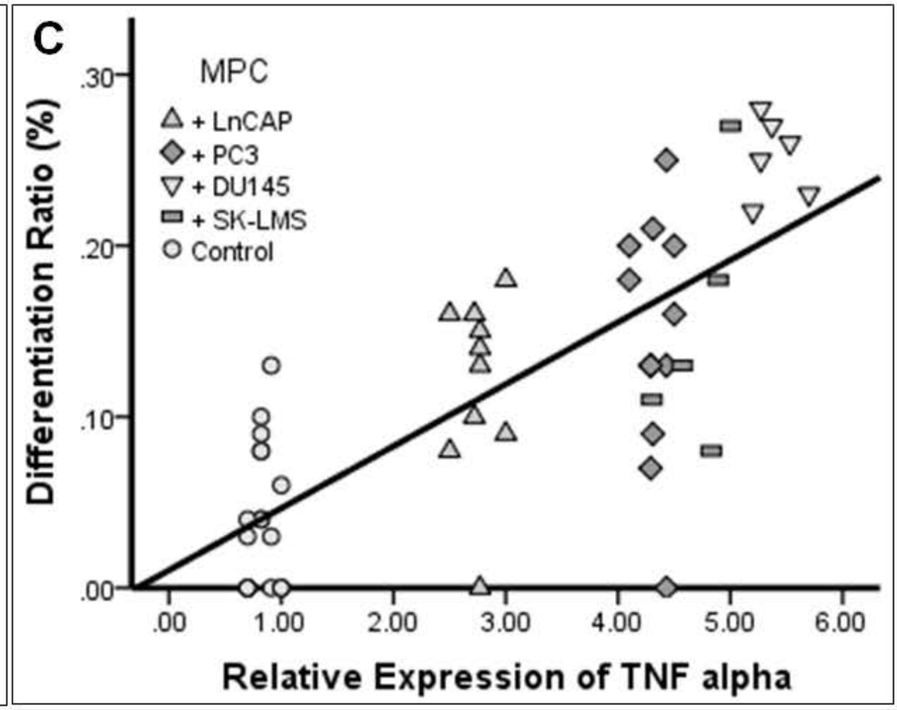
C
MPC
+ LnCAP
+ PC3
+ DU145
+ SK-LMS
Control
Differentiation Ratio (%)
.30
.20
.10
.00
.00
1.00
2.00
3.00
4.00
5.00
6.00
Relative Expression of TNF alpha

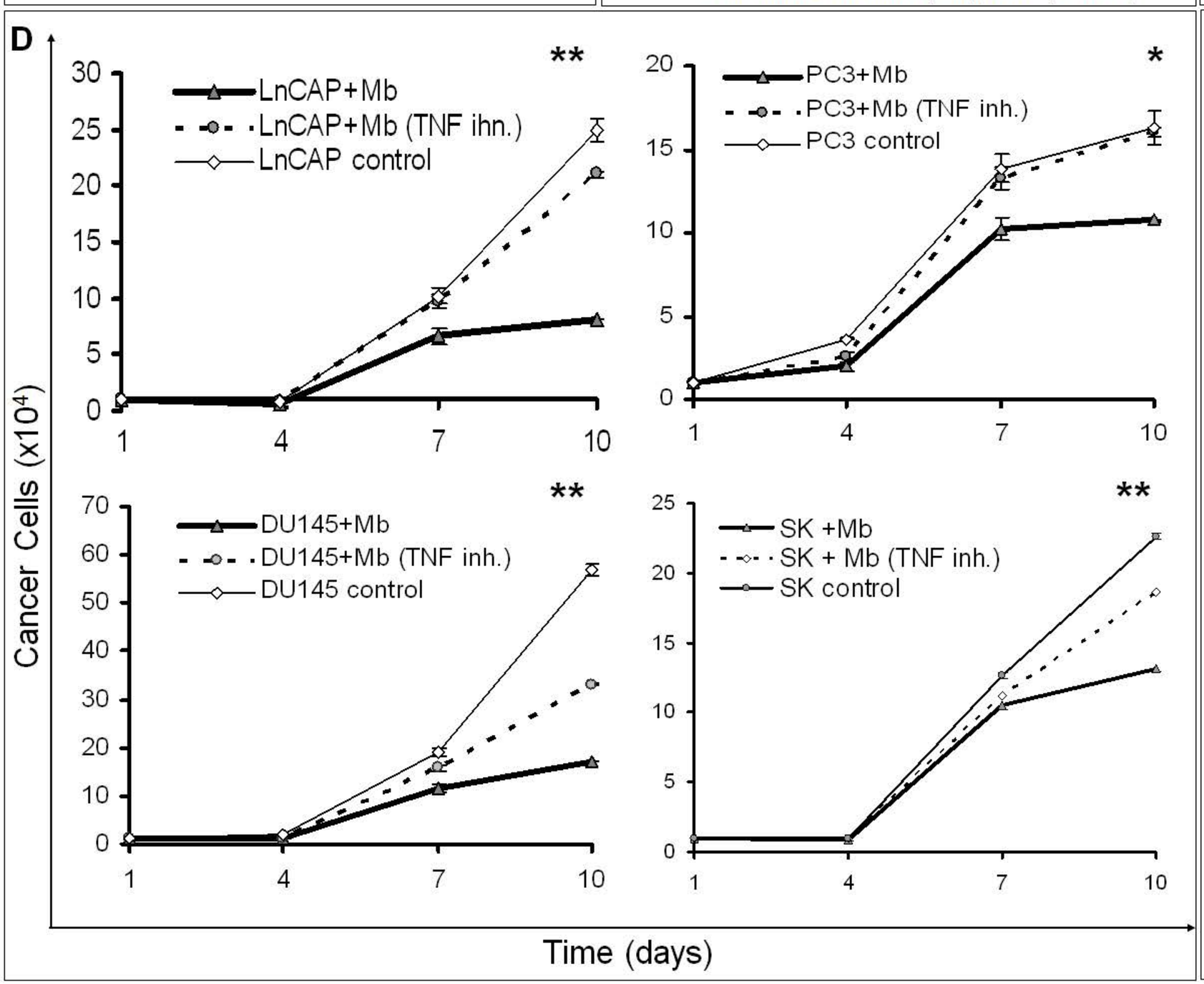
D
LnCAP+Mb
LnCAP+Mb (TNF ihn.)
LnCAP control
PC3+Mb
PC3+Mb (TNF inh.)
PC3 control
DU145+Mb
DU145+Mb (TNF inh.)
DU145 control
SK +Mb
SK + Mb (TNF inh.)
SK control
**
*
**
**
Cancer Cells (x10⁴)
Time (days)

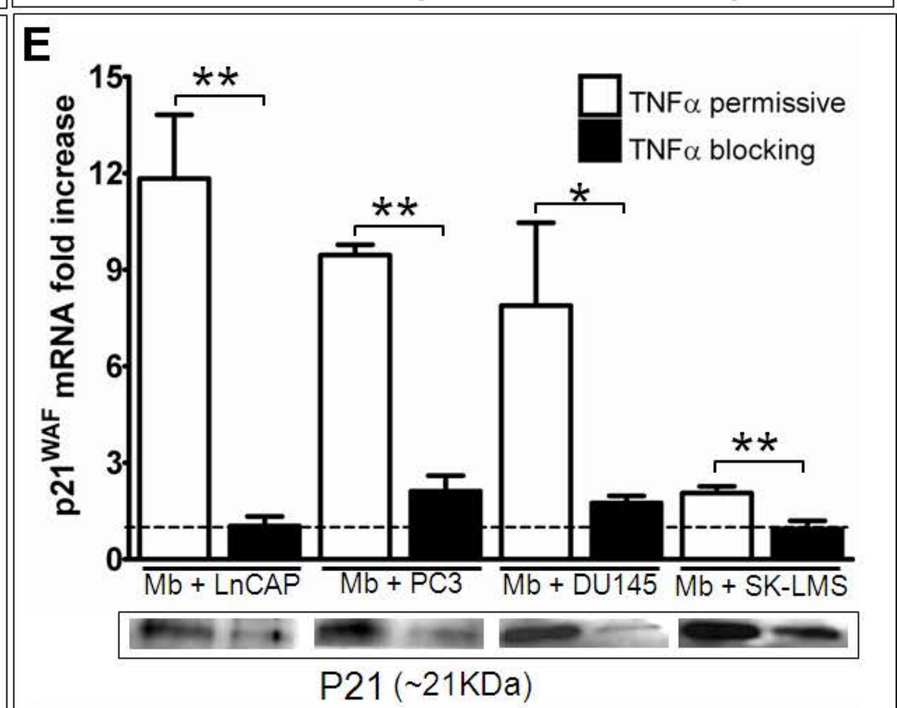
E
TNFα permissive
TNFα blocking
p21WAF mRNA fold increase
Mb + LnCAP
Mb + PC3
Mb + DU145
Mb + SK-LMS
P21 (~21KDa)

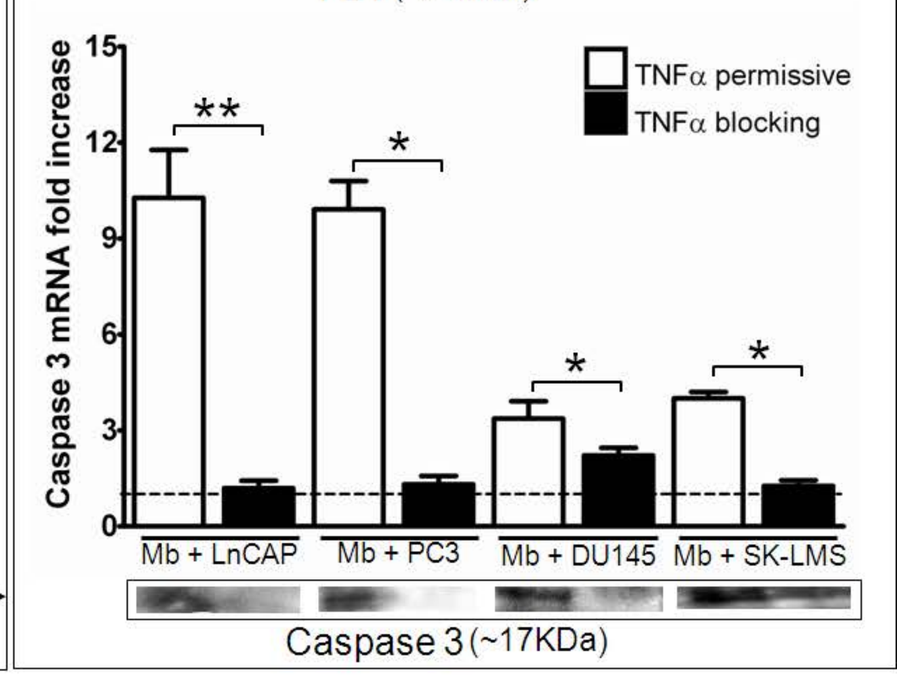
TNFα permissive
TNFα blocking
Caspase 3 mRNA fold increase
Mb + LnCAP
Mb + PC3
Mb + DU145
Mb + SK-LMS
Caspase 3 (~17KDa)

A

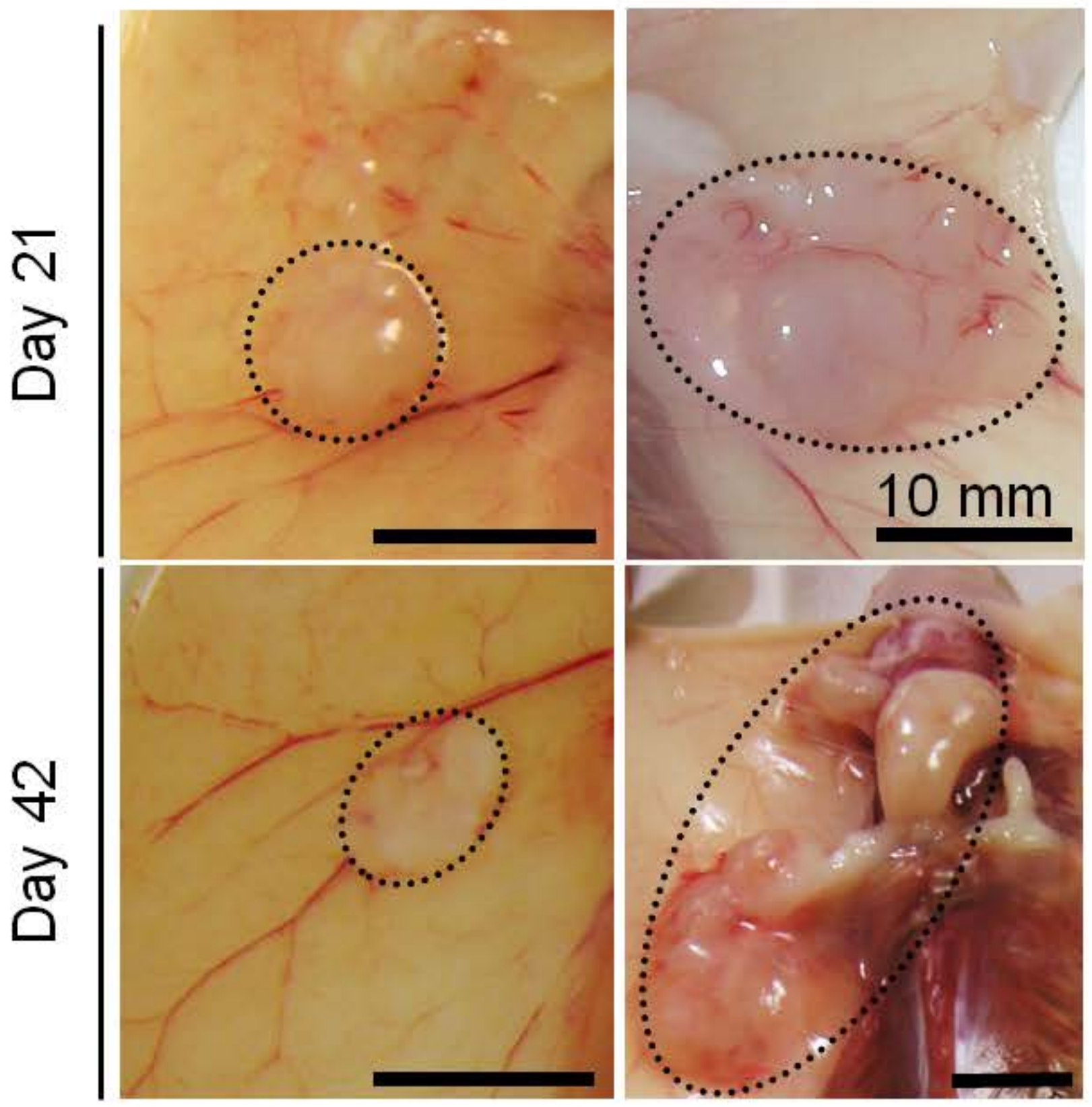
DU145 + Mb
DU145 control
Day 21
Day 42
10 mm

B

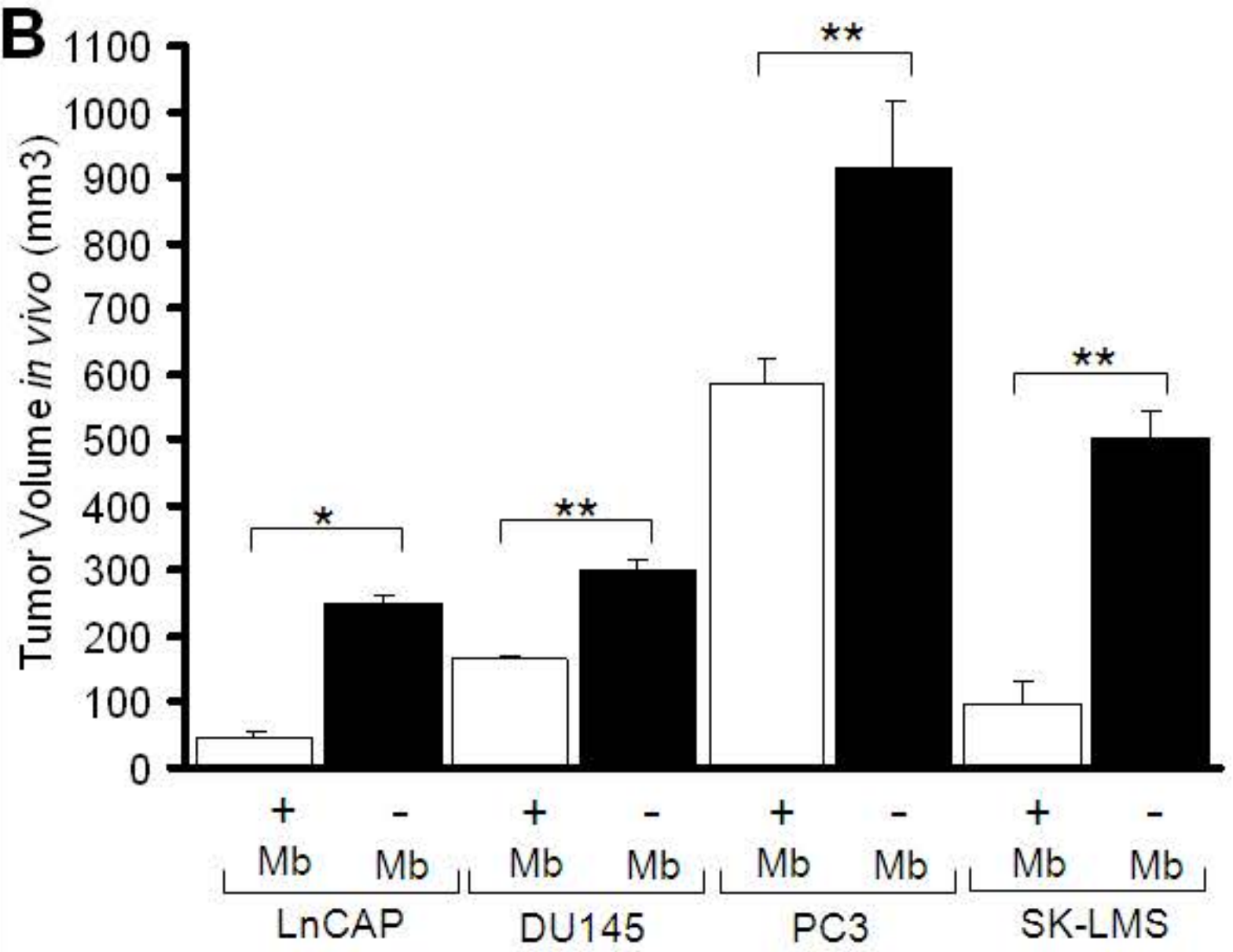
Tumor Volume in vivo (mm3)
1100
1000
900
800
700
600
500
400
300
200
100
0
*
**
**
**
+ - + - + - + -
Mb Mb Mb Mb Mb Mb Mb Mb
LnCAP
DU145
PC3
SK-LMS

C

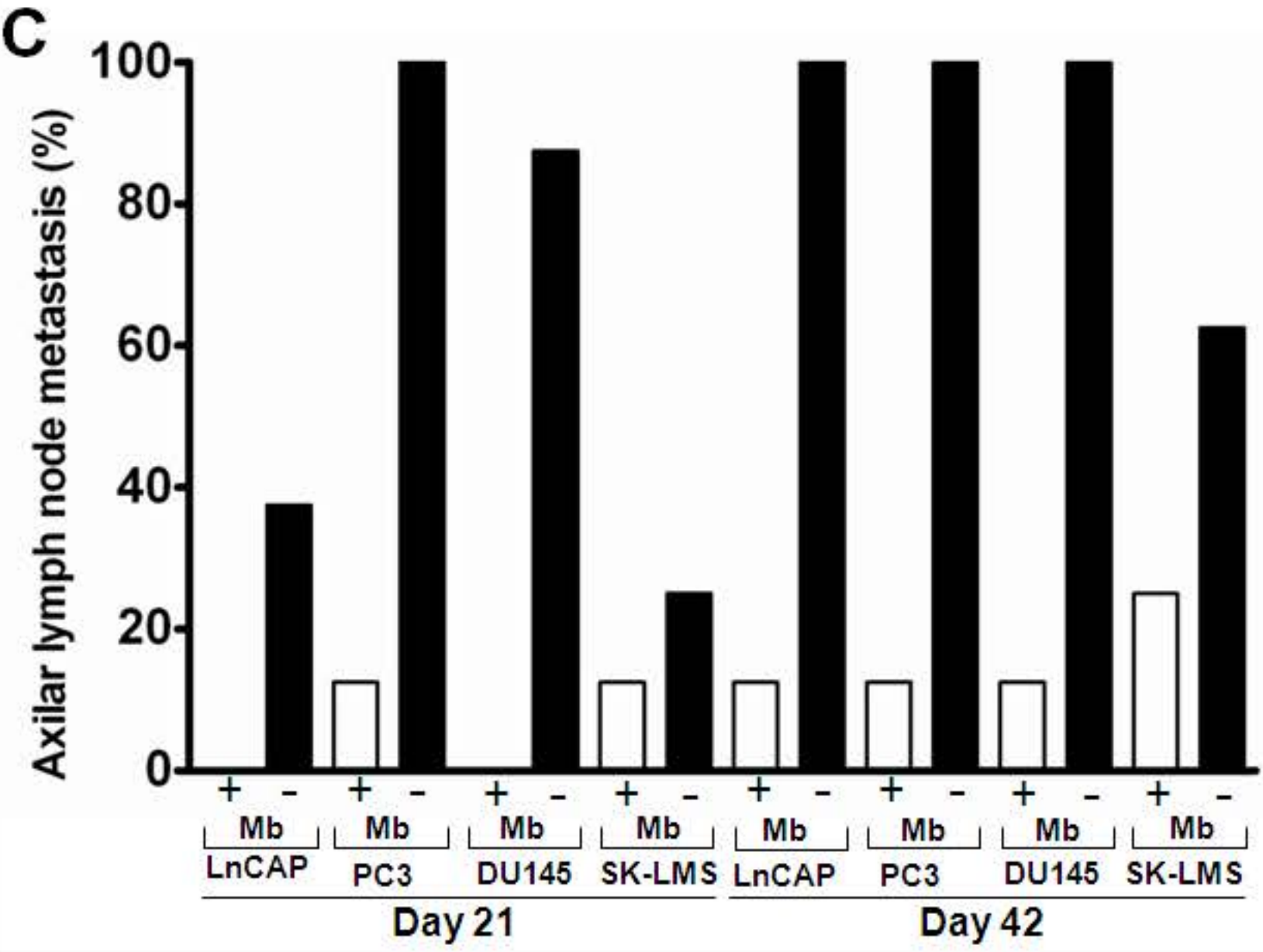
Axilar lymph node metastasis (%)
100
80
60
40
20
0
+ - + - + - + - + - + - + - + -
Mb Mb Mb Mb Mb Mb Mb Mb Mb Mb Mb Mb Mb Mb Mb Mb
LnCAP PC3 DU145 SK-LMS LnCAP PC3 DU145 SK-LMS
Day 21
Day 42

LnCAP
PC3
DU145
SK.LMS
H&E
+ Mb
-Mb
M
C
250 µm
p21WAF
Caspase 3
0 µm 100
0 µm 50

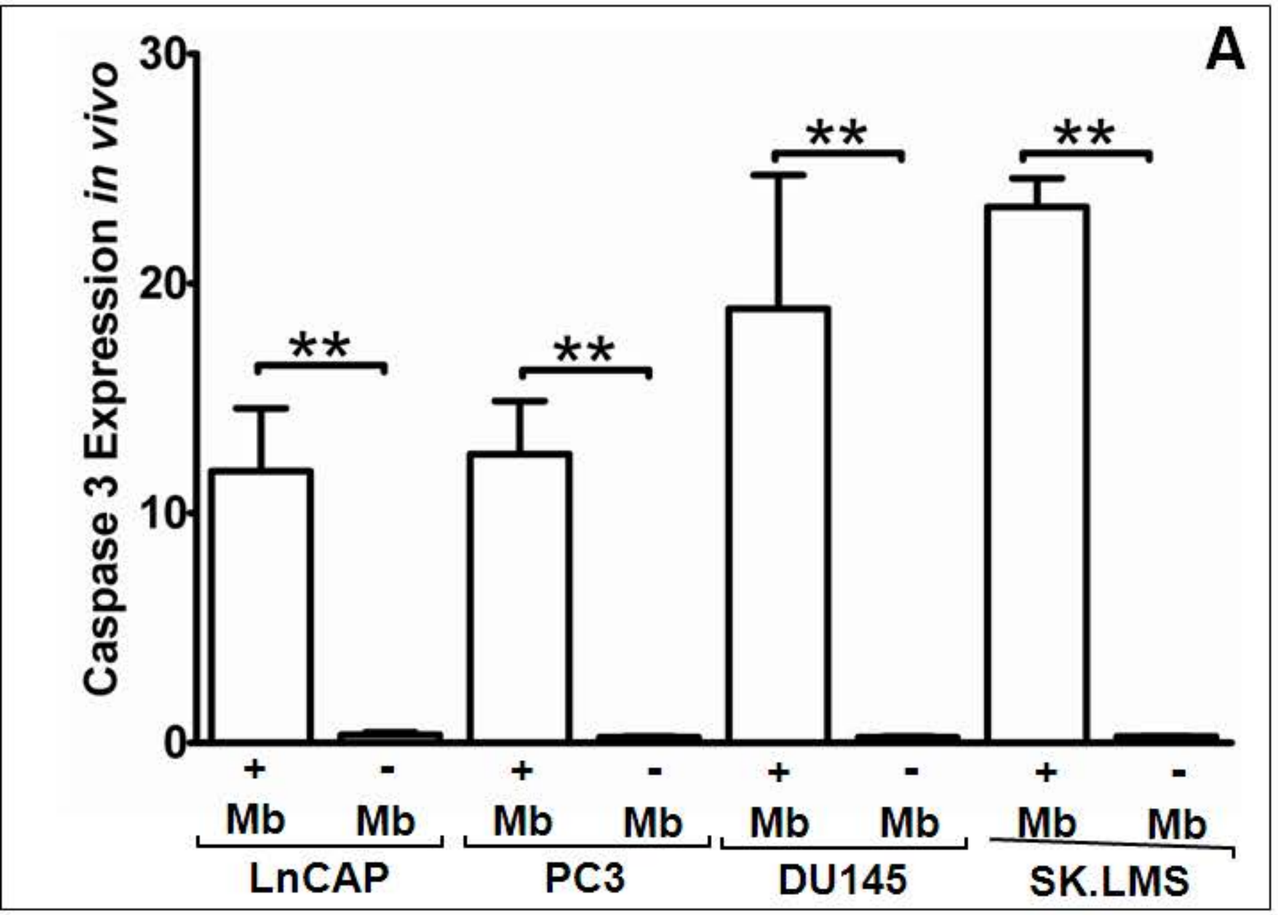
A
Caspase 3 Expression in vivo
30
20
10
0
**
**
**
**
+
-
+
-
+
-
+
-
Mb
Mb
Mb
Mb
Mb
Mb
Mb
Mb
LnCAP
PC3
DU145
SK.LMS

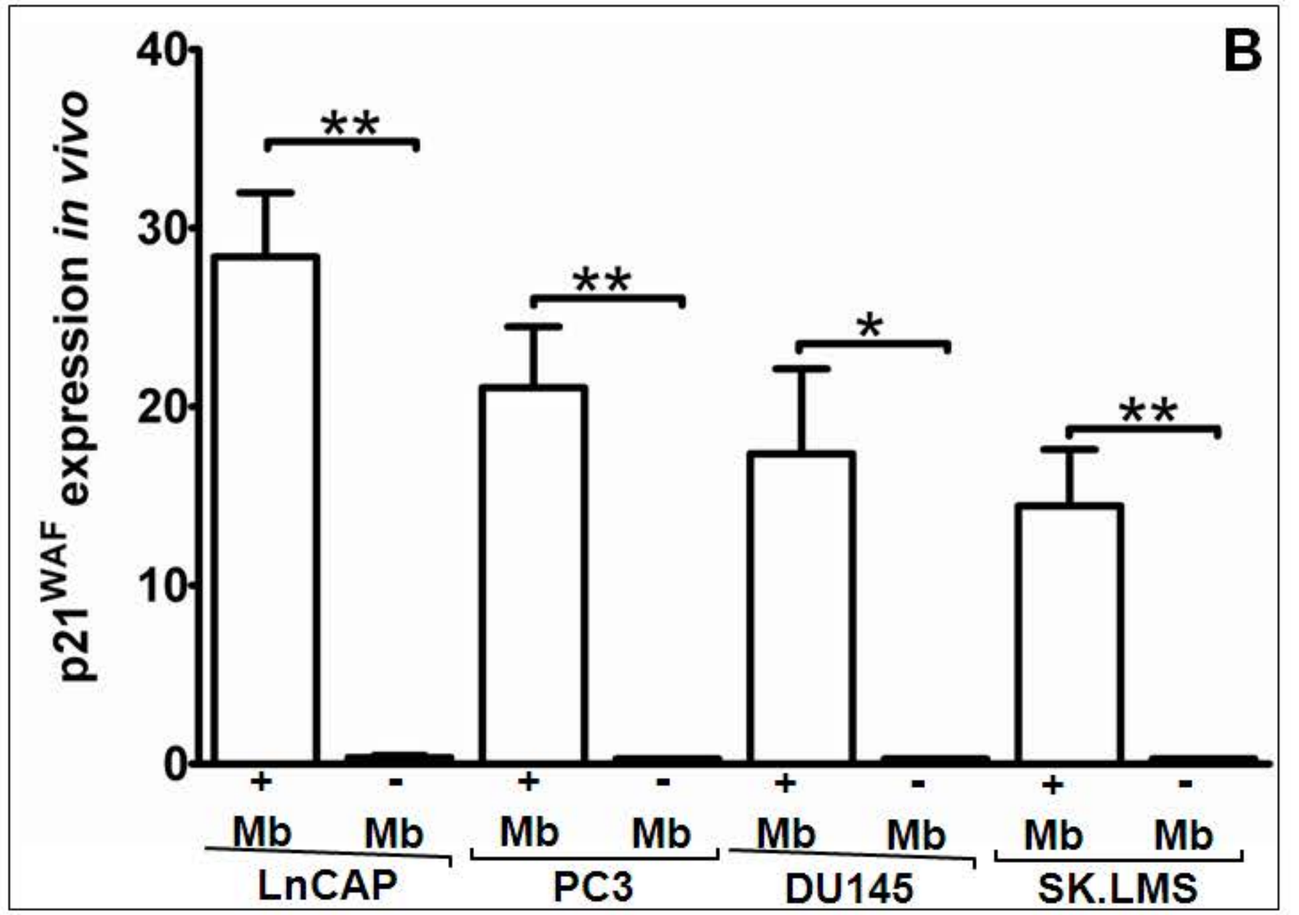
B
p21WAF expression in vivo
40
30
20
10
0
**
**
*
**
+
-
+
-
+
-
+
-
Mb
Mb
Mb
Mb
Mb
Mb
Mb
Mb
LnCAP
PC3
DU145
SK.LMS

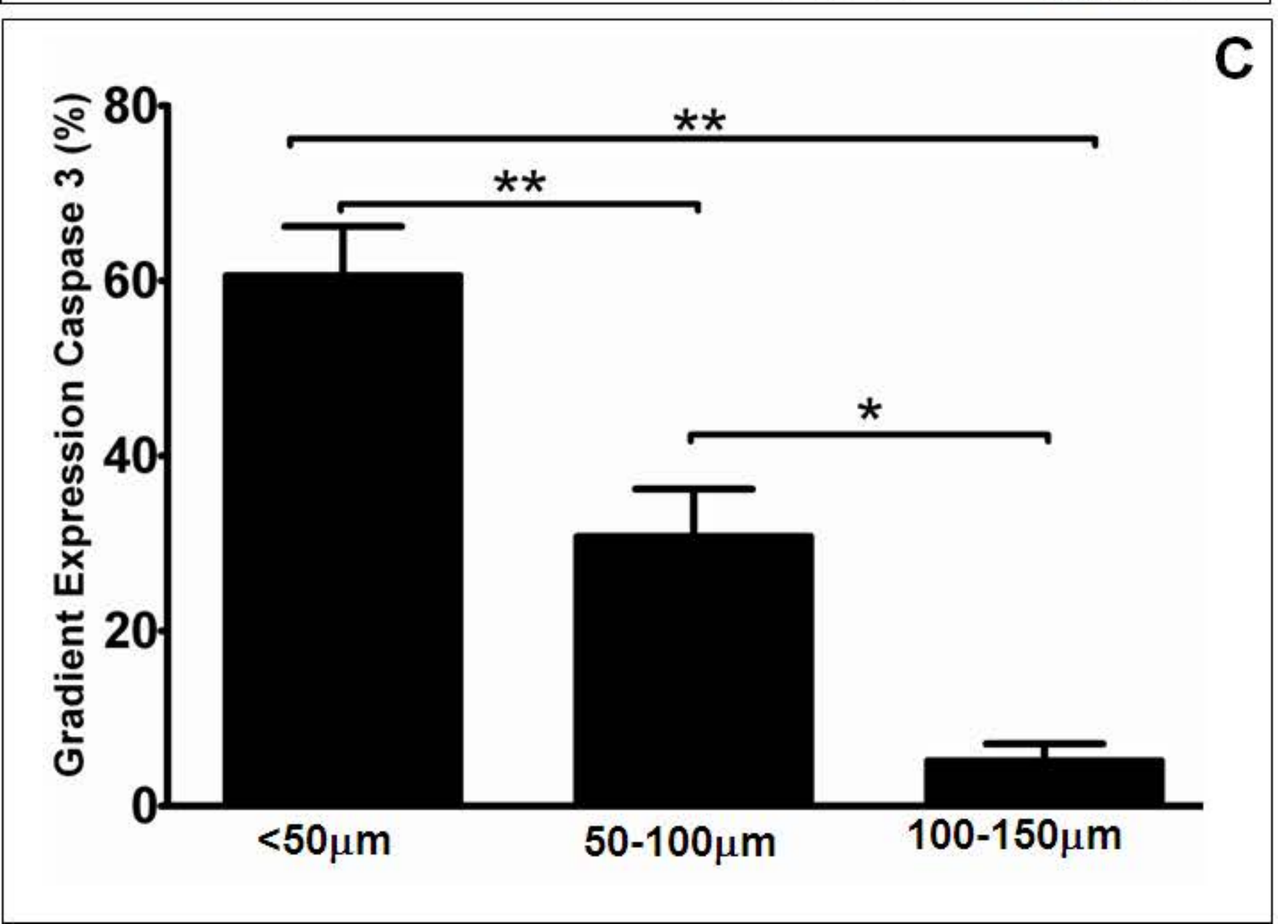
C
Gradient Expression Caspase 3 (%)
80
60
40
20
0
**
**
*
<50µm
50-100µm
100-150µm

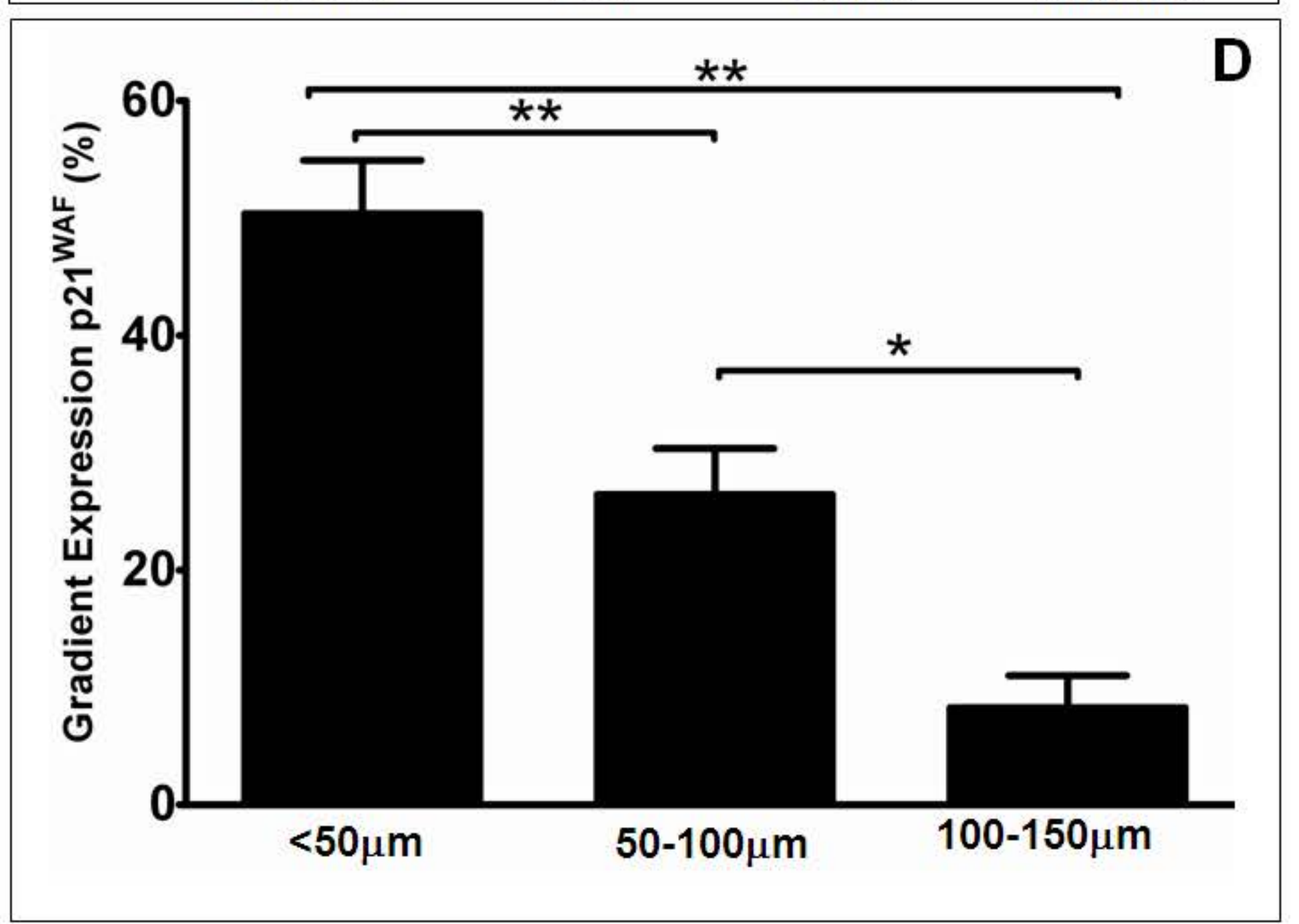
D
Gradient Expression p21WAF (%)
60
40
20
0
**
**
*
<50µm
50-100µm
100-150µm